



## Fabrication of cm scale buckypapers of horizontally aligned multiwall carbon nanotubes highly filled with Fe<sub>3</sub>C: the key roles of Cl and Ar-flow rate

Received 00th January 20xx,  
Accepted 00th January 20xx

Filippo S.Boi<sup>a,c\*</sup>, Jian Guo<sup>a</sup>, Shanling Wang<sup>b</sup>, Yi He<sup>b</sup>, Gang Xiang<sup>a</sup>, Xi Zhang<sup>a\*\*</sup> and Mark Baxendale<sup>c\*\*\*</sup>

DOI: 10.1039/x0xx00000x

www.rsc.org/

**A key challenge in the fabrication of ferromagnetically filled carbon-nanotube buckypapers in presence of Cl-radicals is the achievement of a preferential horizontal nanotube-alignment. We show that a horizontal-alignment can be achieved by tuning two main CVD parameters for a fixed dichlorobenzene concentration: the precursor-evaporation temperature and the flow rate.**

For more than a decade carbon nanotubes (CNTs) filled with ferromagnetic materials like  $\alpha$ -Fe and Fe<sub>3</sub>C have been an important focus of research owing to their high chemical stability, tuneable anisotropies, high saturation magnetizations and coercivities<sup>1-21</sup>. These nanostructures are generally grown in the form of partially filled vertically aligned films through a method known as chemical vapour deposition (CVD) in which one or more metallocene precursors are evaporated and pyrolysed on the top of smooth Si/SiO<sub>2</sub> substrates<sup>1-21</sup>. In particular the control of CNTs filling rate has posed many challenges owing to the fixed Fe:C (1:10) ratio of the metallocenes precursors. Recent reports have shown that the use of low vapour flow rates can be very useful for the promotion of high CNTs filling rates in radial structures produced in viscous boundary layers<sup>22</sup>, in flower-like structures produced by homogeneous nucleation in perturbed CVD<sup>23</sup> and in vertically aligned CNT-films where the length of the encapsulated  $\alpha$ -Fe ferromagnet can be enhanced by using low vapour flow rates and controlled evaporation rates as shown by Peci et al.<sup>24</sup>. Instead the use of high vapour flow rates has been reported to create discontinuities in the CNTs  $\alpha$ -Fe filling<sup>25</sup>.

Differently, the control of filled CNTs alignment in a horizontal direction is still a strong challenge. Recent works have shown that mixture of single or mixed metallocenes with Cl-containing hydrocarbons can allow the fabrication of very elastic membranes known as buckypapers which comprise entangled CNTs highly filled with Fe<sub>3</sub>C or other alloys<sup>26-33</sup>. The Cl radicals can enhance the carbon nanotubes filling rates through the formation of CCl<sub>4</sub> species which can remove carbon feedstock from the pyrolyzing system and can slow down the CNT growth and filling processes by chemically etching the catalyst surface. The highly tuneable magnetic properties and high flexibility demonstrated in literature make these films suitable candidates for numerous applications as flexible ferromagnetic electrodes, actuators, field emission devices, artificial muscles, organic vapour sorbents, hydrogen storage systems, fire retardancy and many others<sup>26-35</sup>. However, ultimately, the properties of these films could be further enhanced by controlling both the alignment and filling rate of the CNTs comprised in the buckypaper, opening new avenues toward the development of flexible data storage devices, actuator devices, flexible exchange bias devices and other spin-based type devices. In this paper we show that such control of CNTs alignment can be achieved by tuning two main parameters of the CVD system for a fixed dichlorobenzene concentration: the evaporation temperature of the precursor and the vapour flow rate. Through scanning electron microscopy (SEM) and backscattered electrons (BE) we show that the alignment of the nanotubes increases with the vapour flow rate at which the ferrocene/dichlorobenzene mixture is delivered in the decomposition zone of the CVD system. Also we show that the size of the bucky-paper is strongly dependent on the evaporation temperature of the precursor-mixture and increases with the decrease of the evaporation temperature

<sup>a</sup> College of Physical Science and Technology Sichuan University, Chengdu China.

<sup>b</sup> Analytical and Testing Centre Sichuan University Chengdu China.

<sup>c</sup> School of Physics and Astronomy Queen Mary University of London.

Email first corresponding author: f.boi@scu.edu.cn

Email second corresponding author: xizhang@scu.edu.cn

Email third corresponding author: m.baxendale@qmul.ac.uk

DOI: 10.1039/x0xx00000x

from 120 °C to the value of 90 °C. Attempts to use higher evaporation temperatures led to the formation of amorphous carbon and small quantities of iron-chloride due to the high concentration of Cl in the reactor. The crystal structure and composition of the as grown buckypapers is investigated through X-ray- diffraction (XRD) and - photoelectron spectroscopy (XPS). The metal content is investigated through thermogravimetric analyses (TGA). The magnetic properties of the buckypapers grown at different evaporation temperature and flow rate are investigated through vibrating sample magnetometry (VSM). The metallicity and the degree of horizontal alignment within a typical aligned CNTs buckypaper are investigated through Seebeck coefficient measurements (see supp info for detailed experimental section). The morphology of the cm-size (1.5 cm X 1.5 cm) buckypapers obtained with an evaporation temperature of 120 °C was firstly revealed by SEM analyses. Fig.1 shows a top view with an increasing level of detail of a buckypaper obtained with an evaporation temperature of 120 °C and an Ar flow rate of 100 mL/min. The CNTs comprised in the buckypaper are found to be highly aligned in one direction which can be identified as that of the Ar flow during the growth in the CVD reactor. The high alignment is shown in Fig.1A-C with an increasing detail. The investigations of the filling rate with BE revealed that continuous filling is present in the CNTs (Fig.1D). This was also confirmed by TEM measurements. A top view of single filled CNTs analysed through TEM is shown in Fig.2A-B while a high detail of the encapsulated crystals is shown in Fig.2C-D with high resolution. The observed lattice spacings of 0.4 nm and 0.5 nm correspond to those of Fe<sub>3</sub>C single crystals (100 and 001 reflections) with space group Pnma. Interestingly in the region of CNT-closure a decrease in the CNT-walls number is found (see yellow and magenta arrows).

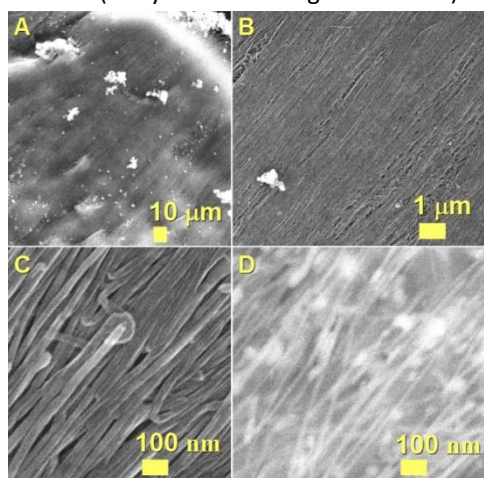


**Figure 1:** SEM micrographs (A-C) showing the high alignment of the CNTs comprised in the buckypaper obtained with vapour flow rate of 100 mL/min and evaporation

temperature of 120 °C. In D the very high filling rate of the CNTs is shown with high detail.

This can be associated to the etching behaviour of the Cl-radicals during the CNT-growth process.

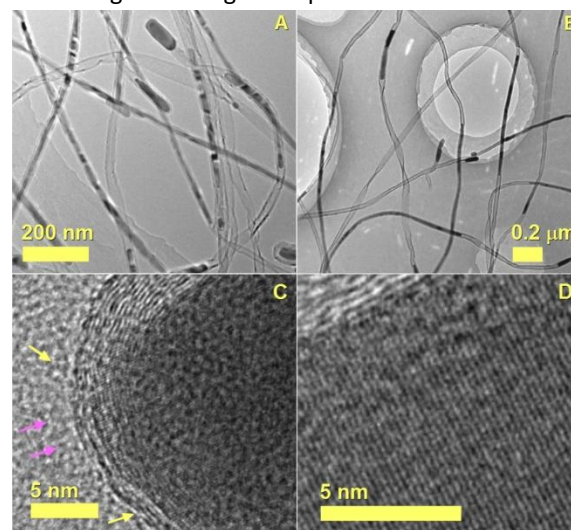


**Figure 2:** TEM micrographs (A-B) and HRTEM micrographs (C-D) showing the Fe<sub>3</sub>C-filling rates of the CNTs obtained with a flow rate of 100 mL/min and evaporation temperature of 120 °C.

A different morphology was found in the buckypapers (dimensions of 1.5 cm X 1.5 cm) obtained with an evaporation temperature of 120 °C and an Ar flow rate of 20 mL/min. As shown in Fig.supp 1 with a systematic increase of detail (Fig. supp 1 A-C) in these conditions the CNTs alignment is lost and the CNTs within the buckypaper have a random orientation. Also in this case BE analyses (see Fig. Supp.1B) revealed high filling rates of the CNTs capillary (bright areas). These observations confirm the key role played by the vapour flow rate in the control of the CNTs horizontal alignment. A higher detail of morphology, filling rate and structure of these CNTs obtained with a flow rate of 20 mL/min is shown also in the TEM and HRTEM micrographs in Fig. Supp 2. As for the aligned CNTs buckypaper, also in this case the observed encapsulated crystals corresponded to the Fe<sub>3</sub>C phase, however a lower filling rate is observed. In order to further confirm the presence of Fe<sub>3</sub>C as a single phase in the sample, further analyses were performed with XRD. As shown in Fig.Supp3 the XRD analyses performed in both the types of samples produced with flow rates of 100 mL/min and 20 mL/min revealed the presence of a single phase of Fe<sub>3</sub>C with space group Pnma characterized by preferred orientations. These results were also confirmed by Raman and XPS measurements (see supp info Figs 4-5) which also revealed the presence of oxygen impurities probably adsorbed in the buckypaper pores (see supp info Figs 5-6) . Note that the size of the produced buckypapers could be further increased to that of 1.5 cm (width) X 3.5 cm (length)

by decreasing the evaporation temperature of the precursors to 90 °C without changing the structure of the encapsulated crystals which remained that of Fe<sub>3</sub>C with space group Pnma. This size-change can be explained by considering that the use of a lower evaporation temperature allows a lower rate of dichlorobenzene evaporation and therefore a lower concentration of Cl radicals in the pyrolysing system. In our experiments we find that in conditions of low Cl-radicals concentrations almost no residues of metal chloride are found in the CVD system, suggesting that in such conditions the formation of CCl<sub>4</sub> species is more probable. This observation explains why the use of low evaporation temperatures of 120 °C, 90 °C or lower is crucial. Note that the XPS analyses of the aligned CNTs buckypapers excluded the presence of Cl residues in the samples. Instead if the evaporation temperature is increased up to 220 °C, owing to the higher concentration of Cl species in the system, only metal-chloride phases and amorphous carbon will be obtained as product. The metal-based filling content of the CNTs was then investigated. As shown in Fig.3 (A-B) the TGA analyses revealed an extremely high metal content inside the CNTs. The measured filling content in the case of the buckypapers of aligned CNTs produced with vapour flow rate of 100 mL/min is comparable with that obtained with a lower flow rate. The highest metal content (50.9 %) was obtained when the evaporation temperature of 90 °C and the vapour flow rate of 20 mL/min were used. The measured metal content is also comparable to those observed in the previous reports on filled-CNTs produced in presence of Cl radicals<sup>26-32</sup>. The magnetic properties were also investigated with VSM at room temperature. As shown in Fig.4 the obtained saturation magnetizations values of 57.8 emu/g (red hysteresis), 39.1 emu/g (blue hysteresis), 25.4 emu/g (black hysteresis) and 23.9 emu/g (green hysteresis) are comparable to those reported in literature for large size Fe<sub>3</sub>C-filled buckypapers<sup>26</sup>. It is interesting to notice that the saturation magnetization of the aligned-CNTs buckypapers obtained with a vapour flow rate of 100 mL/min decreases when the evaporation temperature is decreased to 90 °C. Instead for the CNTs buckypapers obtained with vapour flow rates of 20 mL/min an increase in the saturation magnetization is found. This is in agreement with the TGA analyses outlined above. The measured coercivities were instead similar for all the buckypapers-type (500 Oe). The Seebeck coefficient was measured to assess the metallicity and the degree of horizontal alignment within a typical aligned CNTs buckypaper using the analysis of thermoelectric behaviour of aligned and randomly oriented CNT networks by Baxendale et al<sup>36</sup>. The linear relationship

between Seebeck coefficient and temperature, Fig.5, is a strong indicator of both the metallicity that results from the graphitic CNT walls and a high degree of horizontal alignment of individual CNTs.

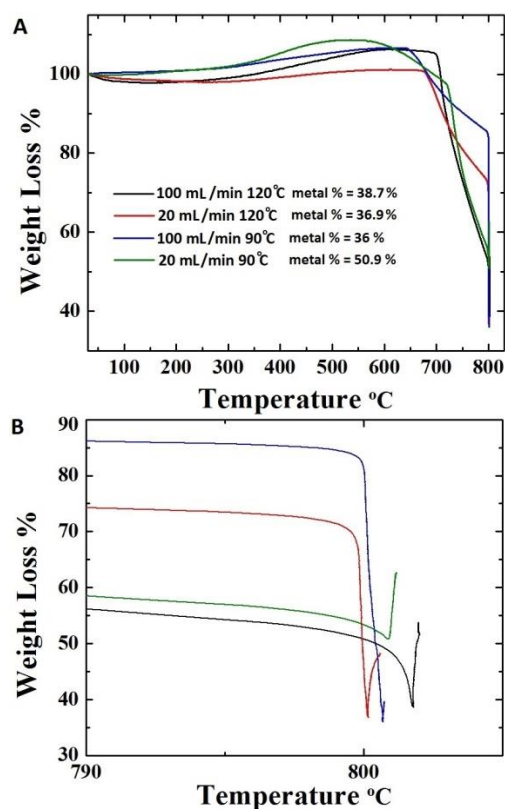


Figure 3: TGA analyses of the buckypaper produced with evaporation temperatures of 90 and 120 °C and vapour flow rates of 20 and 100 mL/min.

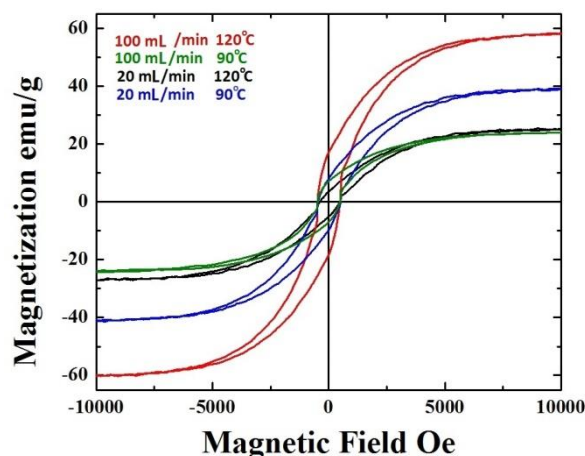


Figure 4: Hysteresis loops measured at room temperature in the buckypapers produced with evaporation temperatures of 90 and 120 °C and vapour flow rates of 20 mL/min and 100 mL/min.

## Conclusions

In conclusion we have shown an advanced CVD method which allows the fabrication of buckypapers comprising CNTs highly filled with Fe<sub>3</sub>C characterized by a high horizontal alignment. This result is achieved by tuning (for a fixed

dichlorobenzene concentration) two main parameters: the evaporation temperature and the vapour flow rate.

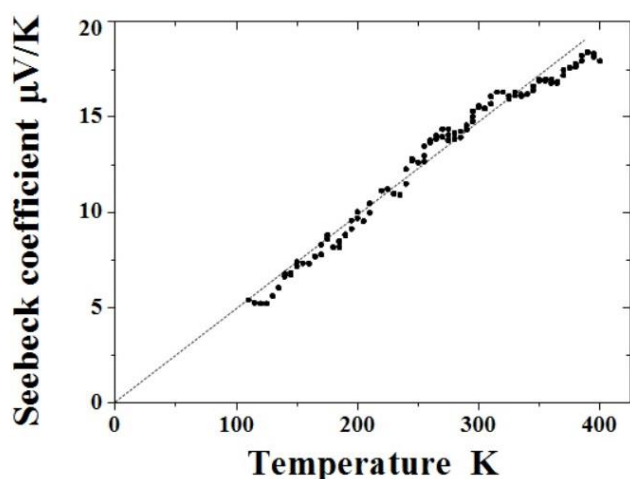


Figure 5: The temperature dependence of Seebeck coefficient of a typical buckypaper. The observed linear, through-the-origin characteristic is a strong indicator of both the metallicity that results from the electronic band structure of graphitic carbon and a high degree of horizontal alignment of individual CNTs in the buckypaper<sup>34</sup>. The dotted line is a guide to the eye.

#### Notes and references

We acknowledge Prof. Gong Min for his continuous support and the National Natural Science Foundation of China Grant No 11404227.

- 1 A. L. Danilyuk, A. L. Prudnikava, I. V. Komissarov, K. I. Yanushkevich, A. Derory, F. Le Normand, V. A. Labunov, S. L. Prischepa. *Carbon*, 2014, **68**, 337.
- 2 I. Monch, A. Leonhardt, A. Meye, S. Hampel, R. Kozhuharova-Koseva, D. Elefant, M. P. Wirth and B. Buchner. *J. Phys.: Conf. Ser.* 2007, **61**, 820–824.
- 3 H. Reuther, C. Muller, A. Leonhardt and M. C. Kutz. *J. Phys.: Conf. Ser.* 2010, **217**, 012098.
- 4 O. V. Kharissova, M. Garza Castañón, J. L. Hernández Pinero, U. Ortiz Méndez and B. I. Kharisov. *Mech. Adv. Mater. Struc.* 2009, **16**, 63–68.
- 5 S. Groudeva-Zotova, R. Kozhuharova, D. Elefant, T. Muhl, C. M. Schneider, I. Monch. *J. Magn. Magn. Mater.* 2006, **306**, 40–50.
- 6 A. L. Elias, J. A. Rodríguez-Manzo, M. R. McCartney, D. Golberg, A. Zamudio, S. E. Baltazar, F. Lopez-Urias, E. Muñoz-Sandoval, L. Gu, C. C. Tang, D. J. Smith.; Y. Bando, H. Terrones, M. Terrones. *Nano Lett.*, 2005, **5**, 467.
- 7 A. Morelos-Gomez, F. Lopez-Urias, E. Muñoz-Sandoval, C. L. Dennis, R. D. Shull, H. Terrones and M. Terrones. *J. Mater. Chemist.* 2010, **20**, 5906.
- 8 D. Golberg, M. Mitome, Ch. Muller, C. Tang, A. Leonhardt, Y. Bando. *Act. Mater.*, 2006, **54**, 2567.
- 9 F. C. Dillon, A. Bajpai, A. Koos, S. Downes, Z. Aslam, N. Grobert *Carbon*, 2012, **50**, 3674.
- 10 H. Terrones, F. López-Urías, E. Muñoz-Sandoval, J. A. Rodríguez-Manzo, A. Zamudio, A. L. Elías, et al. *Sol. Stat. Sci.*, 2006, **8**, 303.
- 11 S. Hampel, A. Leonhardt, D. Selbmann, K. Biedermann, D. Elefant, Ch. Muller, T. Gemming and B. Buchner. *Carbon*, 2006, **44**, 2316.
- 12 A. Leonhardt, M. Ritschel, M.; Elefant, D. N. Mattern, K. Bie-

dermann, S. Hampel, Ch. Muller, T. Gemming, B. Buchner.

- J. Appl. Phys.*, 2005, **98**, 074315.
- 13 A. Leonhardt, M. Ritschel, R. Kozhuharova, A. Graff, T. Muhl, R. Huhle, I. Monch, D. Elefant and C. M. Schneider. *Diam. Relat. Mater.*, 2003, **12**, 790.
  - 14 N. Grobert, M. Mayne, M. Terrones, J. Sloan, R. E. Dunin-Borkowski, R. Kamalakaran, T. Seeger, H. Terrones, M. Ruhle, D. R. M. Walton, H. W. Kroto and J. L. Hutchison. *Chem. Comm.*, 2001, **5**, 471–2.
  - 15 U. Weissker, S. Hampel, A. Leonhardt, B. Buchner. *Materials* 2010, **3**, 4387.
  - 16 F. S. Boi, G. Mountjoy, Z. Luklinska, L. Spillane, L. S. Karlsson, R. M. Wilson, A. Corrias, M. Baxendale. *Microsc. and Microanal.* 2013, **19**, 1298.
  - 17 C. Muller, D. Golberg, A. Leonhardt, S. Hampel, B. Buchner. *Phys. Stat. sol. (a)*, 2006, **203**, 1064.
  - 18 C. Muller, S. Hampel, D. Elefant, K. Biedermann, A. Leonhardt, M. Ritschel, B. Buchner. *Carbon*, 2006, **44**, 1746.
  - 19 S. Karmakar, S. M. Sharma, M. D. Mukadam, S. M. Yusuf, A. K. Sood. *J. Appl. Phys.*, 2005, **97**, 054306.
  - 20 J. F. Marco, J. R. Gancedo, A. Hernando, P. Crespo, C. Prados, J. M. Gonzalez N. Grobert, M. Terrones, D. R. M. Walton and H. W. Kroto. *Hyperf. Interact.*, 2002, **139**, 535.
  - 21 C. Prados, P. Crespo, J. M. Gonzalez, A. Hernando, J. F. Marco, R. Gancedo, N. Grobert, M. Terrones, R. M. Walton and H. W. Kroto. *Phys. Rev. B*, 2002, **65**, 113405.
  - 22 F. S. Boi, G. Mountjoy, M. Baxendale. *Carbon*, 2013, **64**, 516.
  - 23 F. S. Boi, G. Mountjoy, R. M. Wilson, Z. Luklinska, L. J. Sawiak, M. Baxendale. *Carbon*, 2013, **64**, 351–8.
  - 24 T. Peci, M. Baxendale. *Carbon*, 2015, **98**, 519–25.
  - 25 F. S. Boi, S. Maugeri, J. Guo, M. Lan, S. Wang, J. Wen, G. Mountjoy, M. Baxendale, G. Nevill, R. M. Wilson, Y. He, S. Zhang, and G. Xiang *Appl. Phys. Lett.*, 2014, **105**, 243108.
  - 26 R. Lv, S. Tsuge, X. Gui, K. Takai, F. Kang, T. Enoki, J. Wei, J. Gu, K. Wang, D. Wu. *Carbon*, 2009, **47**, 1141.
  - 27 W. Wang, K. Wang, R. Lv, W. J. Zhang, X. Kang, F. Chang, J. Chang, Q. Shu, Y. Wang, D. Wu. *Letters to the Editor Carbon*, 2007, **45**, 1105–36.
  - 28 R. Lv, F. Kang, J. Gu, X. Gui, J. Wei, K. Wang and D. Wu. *Appl. Phys. Lett.*, 2008, **93**, 223105.
  - 29 J. Cheng, X. P. Zou, G. Zhu, M. F. Wang, Y. Su, G. Q. Yang, X. M. Lu. *Sol. St. Comm.*, 2009, **149**, 1619–22.
  - 30 X. Gui, K. Wang, W. Wang, J. Wei, X. Zhang, R. Lv, Y. Jia, Q. Shu, F. Kang, D. Wu. *Mater. Chem. Phys.*, 2009, **113**, 634–637.
  - 31 R. Lv, F. Kang, W. Wang, J. G. J. Wei, K. Wang, D. Wu. *Carbon*, 2007, **45**, 1433.
  - 32 R. Lv, A. Cao, F. Kang, W. Wang, J. Wei, J. Gu. *J. Phys. Chem. C*, 2007, **111**, 11475.
  - 33 J. Guo, M. Lan, S. Wang, Y. H, S. Zhang, G. Xiang. *Phys. Chem. Chem. Phys.*, 2015, **17**, 18159.
  - 34 Y. Li and M. Kröger. *Carbon*, 2012, **50**, 1793–1806.
  - 35 Y. Li and M. Kröger. *Appl. Phys. Lett.*, 2012, **100**, 021907.
  - 36 M. Baxendale, K. G. Lim, G. A. J. Amaratunga. *Phys. Rev. B*, 2000, **61**, 12705–12708.